Am J Physiol Heart Circ Physiol 318: H994–H1007, 2020.
First published March 13, 2020; doi:10.1152/ajpheart.00610.2019.

RESEARCH ARTICLE | *Translational Physiology*

Novel insights into cardiac regeneration based on differential fetal and adult ovine heart transcriptomic analysis

Paola Locatelli,[1]* Mariano N. Belaich,[2]* Ayelén E. López,[1] Fernanda D. Olea,[1] Martín Uranga Vega,[1] Carlos S. Giménez,[1] Jorge Alejandro Simonin,[2] María del Rosario Bauzá,[1] Marta G. Castillo,[1] Luis A. Cuniberti,[1] Alberto Crottogini,[1] Carolina S. Cerrudo,[2]* and Pablo D. Ghiringhelli[2]*

[1]*Instituto de Medicina Traslacional, Trasplante y Bioingeniería (IMETTYB), Universidad Favaloro-CONICET, Buenos Aires, Argentina; and* [2]*Laboratorio de Ingeniería Genética y Biología Celular y Molecular; CONICET, Instituto de Microbiología Básica y Aplicada, Departamento de Ciencia y Tecnología, Universidad Nacional de Quilmes, Buenos Aires, Argentina*

Submitted 17 October 2019; accepted in final form 6 March 2020

Locatelli P, Belaich MN, López AE, Olea FD, Uranga Vega M, Giménez CS, Simonin JA, Bauzá MDR, Castillo MG, Cuniberti LA, Crottogini A, Cerrudo CS, Ghiringhelli PD. Novel insights into cardiac regeneration based on differential fetal and adult ovine heart transcriptomic analysis. *Am J Physiol Heart Circ Physiol* 318: H994–H1007, 2020. First published March 13, 2020; doi:10.1152/ajpheart.00610.2019.—The adult mammalian cardiomyocyte has a very limited capacity to reenter the cell cycle and advance into mitosis. Therefore, diseases characterized by lost contractile tissue usually evolve into myocardial remodeling and heart failure. Analyzing the cardiac transcriptome at different developmental stages in a large mammal closer to the human than laboratory rodents may serve to disclose positive and negative cardiomyocyte cell cycle regulators potentially targetable to induce cardiac regeneration in the clinical setting. Thus we aimed at characterizing the transcriptomic profiles of the early fetal, late fetal, and adult sheep heart by employing RNA-seq technique and bioinformatic analysis to detect protein-encoding genes that in some of the stages were turned off, turned on, or differentially expressed. Genes earlier proposed as positive cell cycle regulators such as cyclin A, cdk2, meis2, meis3, and PCNA showed higher expression in fetal hearts and lower in AH, as expected. In contrast, genes previously proposed as cell cycle inhibitors, such as *meis1*, *p16*, and *sav1*, tended to be higher in fetal than in adult hearts, suggesting that these genes are involved in cell processes other than cell cycle regulation. Additionally, we described Gene Ontology (GO) enrichment of different sets of genes. GO analysis revealed that differentially expressed gene sets were mainly associated with metabolic and cellular processes. The cell cycle-related genes *fam64a*, *cdc20*, and *cdk1*, and the metabolism-related genes *pitx* and *adipoq* showed strong differential expression between fetal and adult hearts, thus being potent candidates to be targeted in human cardiac regeneration strategies.

NEW & NOTEWORTHY We characterized the transcriptomic profiles of the fetal and adult sheep hearts employing RNAseq technique and bioinformatic analyses to provide sets of transcripts whose variation in expression level may link them to a specific role in cell cycle regulation. It is important to remark that this study was performed in a large mammal closer to humans than laboratory rodents. In consequence, the results can be used for further translational studies in cardiac regeneration.

cell cycle; development; heart; ovis aries; transcriptome

INTRODUCTION

Cardiovascular disease is the leading cause of death worldwide (54). In conditions characterized by extensive contractile cell loss, like myocardial infarction, the remaining viable myocardium is progressively substituted by connective tissue, a process known as myocardial remodeling. Because the rate of resident cardiomyocyte (CM) proliferation is low and insufficient to replace the lost ones, cardiac function decreases and heart failure develops (60). Currently, the only therapeutic option for patients with end-stage symptomatic heart failure despite maximal pharmacological treatment is heart transplantation (79). Therefore, cardiac regeneration has emerged as a fundamental scientific objective (63), and several approaches, the majority of them based on stem cell implantation, are being tested in animal models (21, 34) and clinical trials (38, 53).

An alternative approach would be to induce the adult cardiomyocytes to reenter the cell cycle and advance into mitosis and cytokinesis. This requires identifying pro- and anti-mitotic regulatory RNAs (23), proteins, hormones, and other metabolites involved in proliferation pathways (49, 50). Once identified, these molecules may be targeted to achieve efficient yet regulated cardiomyocyte cell cycle reentry (75). This approach would, on one hand, circumvent drawbacks associated with stem cell-based regeneration therapies such as cell survival and engraftment and, on the other hand, preserve electromechanical coupling of the new cells within the physiological syncytium.

In fetal sheep, CMs actively replicate until around *day 100* of gestation. From this time point and until term (*day 145* of gestation), CMs progressively differentiate, become binucleated, and exit the cell cycle (65). To enhance the reliability of extrapolating the experimental results to the human, it is convenient to use large mammalian models, whose features, in terms of lifespan, size, gestation time, and hemodynamic variables, among others, are closer to humans than those of laboratory rodents. Among large mammalian models of heart disease, sheep exhibit several advantages, such as its CM's nuclei (1 to 4), which resemble human's more than pig's (1 to 32 nuclei), a slower growth rate than the pig, and the fact that sheep reach maturity at ~25 kg of weight, avoiding misinterpretations in chamber dimensions along follow-up (35).

* P. Locatelli and M. N. Belaich contributed equally to this work, and C. S. Cerrudo and P. D. Ghiringhelli contributed equally to this work.

Address for reprint requests and other correspondence: P. Locatelli, Universidad Favaloro, Solís 453, C1078AAI, Buenos Aires, Argentina (e-mail: plocatelli@favaloro.edu.ar).

0363-6135/20 Copyright © 2020 the American Physiological Society

Downloaded from journals.physiology.org/journal/ajpheart (168.096.240.002) on May 3, 2021.

In this work, we report the bioinformatic analysis of the whole mRNA transcriptome of the ovine heart at two points of development [90-day gestation fetuses (early fetal heart, EFH) and 130-day gestation fetuses (late fetal heart, LFH)] and in adult sheep (adult heart, AH), providing a comparative analysis of the variation in gene expression with a focus in cell cycle regulation pathways. This analysis provides putative RNA biomarkers for each time point of the heart development assessed as well as possible targets for therapies aimed at cardiac regeneration based on cardiomyocyte proliferation.

MATERIALS AND METHODS

Ethics statement. All experimental animal procedures were carried out in accordance with the *Guide for Care and Use of Laboratory Animals* published by the National Institutes of Health (NIH Publication No. 85-23, revised 1996) and approved by the Laboratory Animal Care and Use Committee (CICUAL) of the Favaloro University.

Animals and sample collection. Corriedale healthy 2 yr-old young adults ($n = 3$; 2 males and 1 female) and fetal sheep of two gestational ages from healthy young pregnant female sheep (90 days of gestation, $n = 3$, all males; and 130 days of gestation, $n = 3$, all females) were euthanized with a propofol overdose (Fresenius Kabi Austria, Graz, Austria) and a bolus injection of potassium chloride. The fetuses were surgically obtained through a standard C-section. The young adults and the pregnant sheep were acquired in a local breeding farm (Estancia San Julian S.A., Entre Rios, Argentina), where the gestation follow-up was performed by echography. The thorax was immediately opened, and the heart was excised and weighted. Samples from the left ventricle were collected and immediately frozen in liquid nitrogen. Samples were stored at −70°C until their use for RNA isolation. Experimental groups were identified as early fetal heart (EFH), late fetal heart (LFH), and adult heart (AH), each containing three biological replicas from three different animals (R1, R2, and R3).

The sex was determined through visual inspection and confirmed by quantitative PCR (qPCR) using primers to detect SRY gene (forward: 5′ CAGACAATCATAGCGCAAACG 3′; reverse: 5′ GCTGCTCTCCCTAACATTTTCC 3′).

RNA isolation, library generation, and sequencing. Total RNA isolation from tissue samples was performed using AllPrep DNA/RNA/miRNA Universal Kit (Qiagen, Hilden, Germany), following the manufacturer's protocol. For mRNA isolation, a PolyATtract mRNA Isolation System (Promega, Madison, WI) was used, following the manufacturer's instructions, and stored at −20°C. The obtained mRNA was immediately certified and quantified by using 2100 Bioanalyzer Instrument and Agilent 2100 Expert Software (Agilent Technologies). The samples with an RIN of ~8 were considered adequate for sequencing. Aliquots of mRNA ($n = 9$; 3 for each timepoint) were delivered to Macrogen Inc. (Seoul, South Korea) for cDNA library construction (TruSeq RNA Sample Prep Kit v2) and Next Generation Sequencing using an Illumina Hiseq4000 platform (100-bp paired-end lane, 550 million reads/lane).

Data processing and analysis. Raw reads of RNA-seq (fastq files) were checked to analyze the quality of them using FastQC (version 0.11.5) (4), and the transcription integrity analysis was performed using the TIN program of the Mississippi Galaxy server (https://mississippi.snv.jussieu.fr/). The transcriptome of *Ovis aries* (Texel) version 4.0 (GCF_000298735.2; 49.705 transcripts) was downloaded from NCBI (https://www.ncbi.nlm.nih.gov/) and filtered to have mRNAs, partial mRNAs, and misc RNAs and then employed as a reference for bioinformatics studies.

The transcript abundances in each experimental sample were shown as "transcripts per million" (TPMs), according to the Salmon pipeline (Galaxy server, https://usegalaxy.org/), with standard parameters and Type index = fmd. (47). The TPM values were then normalized according to the corresponding TPM value of GAPDH mRNA of each replica (TPMn). To facilitate the mathematical analysis, TPMn values lower than $1E^{-5}$ (equivalent to 5 reads) were replaced by a pseudocount value ($1E^{-5}$).

For each transcript, when at least two replicas of each experimental group were over $1E^{-5}$, the gene was classified as ON. When this condition was not achieved, the gene was classified as OFF. For the genes classified as ON, the TPMn values of replicas in each group were used to calculate the average and standard deviation. This analysis allowed for the generation of a database containing all the genes expressed in the three experimental groups. With this, each gene status was determined according to whether it was expressed in one, two, or the three experimental groups. This made it possible to select sets of genes with exclusive expression in an experimental group and others shared between any of the experimental groups. A similar analysis was carried out for the genes previously classified as OFF.

In sets of shared expressed genes, for each of the members, the tendency was inferred using ANOVA-Bonferroni statistical analysis, allowing us to classify them according to the expression level in each experimental group (29).

All of the analyses were performed using filters in Microsoft Excel (2010) datasheets and/or ad hoc scripts.

Gene ontology analysis. The previously obtained gene sets as well as the turned-off genes in the three experimental groups were analyzed using the server of the PANTHER Classification System (http://www.pantherdb.org/) for Gene Ontology (GO) classification (41). A functional classification centered in biological processes and based in the human classification of gene function was performed. Additionally, an analysis to assess the functional enrichment level of each GO term was carried out using the functional annotation clustering tool of DAVID server (https://david.ncifcrf.gov/tools.jsp). For this, the biological process category and *Ovis aries* as a species were selected. The GO terms having P values (enrichment score) of <0.05 were then selected for the illustration as heat maps, using the Heatmap2 program from Galaxy server (https://usegalaxy.org).

Reverse transcription and real-time PCR. For each sample, an aliquot of the first total RNA purification was taken and reverse transcription (High Capacity cDNA Reverse Transcription Kit; Applied Biosystems, Foster City, CA) performed. Real-time PCR (SYBR Select Master Mix; Applied Biosystems) was then carried out (StepOne PCR Real Time System; Thermo Fisher) using sheep-specific primers ad hoc designed to quantify gene expression of *cyclin A* (forward: 5′-TTGATAGGTTTCTTTCATCCATGTCT-3′; reverse: 5′-GCAGCAGTGCCCACAAGTT-3′), *cdk2* (cyclin-dependent kinase 2; forward: 5′-AAGATCGGAGAGGGCACGTA-3′; reverse: 5′-CCACTTCTCCCGTCAACTTGTT-3′), *meis2* (myeloid ecotropic viral integration site 2; forward: 5′-GGGCACCCGTTGTTTCC-3′; reverse: 5′-TCGCCAGCTCGCACTTCT-3′), *meis3* (myeloid ecotropic viral integration site 3; forward: 5′-CATGAGAGCCTGGTTGTTCCA-3′; reverse: 5′-GCGCCAGCTGTTTCTTCTG-3′), *meis1* (myeloid ecotropic viral integration site 1; forward: 5′-AACTGACCAGCCCTCTTGGA-3′; reverse: 5′-GCCATCACCTTGCTCACTGC-3′), *p16* (cdkn2aip; forward: 5′-TGGCTGAAGGCATCAAAGTG-3′; reverse: 5′-GCAACCAGTTCGTCTCTTGTGA-3′), *sav1* (salvador 1; forward: 5′-CGGCACGGTCCAACAATT-3′; reverse: 5′-CATTAGCGCTTGAATCTGGAAGA-3′), *nkx2.5* (nk2 homeobox *5*; forward: 5′-CCTGCCAAGGACCATCGA-3′; reverse: 5′-TCCAGTTCCACCGCCTTCT-3′), *aldolase* (forward: 5′-CCTCTCCTGTGCCAGGAACT-3′; reverse: 5′-TGGTAGAGCGTCTCGTGGAA-3′), *enolase* (forward: 5′-TAAAACTATTGCGCCTGCCC-3′; reverse: 5′-CTTGTTGCCAGCATGAGAGC-3′), *ldhb* (lactate dehydrogenase b; forward: 5′-TTTCAGGGCACAATGGCAAC-3′; reverse: 5′-CCTGCAGTTACCACCACGAT-3′), *ppargc1a* (peroxisome proliferator-activated receptor-γ coactivator 1α; forward: 5′-CAAACTTGCTAGCGGTCCTC-3′; reverse: 5′-TAGCCTCATTCTCGGTGGTC-3′), *adipoq* (adiponectin; forward: 5′-GGCTGTGGACCTTTTCCAGT-3′; reverse: 5′-ATGCTTGGTGAAGGCCAGTT-3′), *pitx* (paired-like homeodomain; forward: 5′-CTTTGGAGCTTGGA-

Downloaded from journals.physiology.org/journal/ajpheart (168.096.240.002) on May 3, 2021.

Table 1. *Experimental groups and sample characteristics*

Experimental group	Tissue	Library Type	No. of Libraries	Total Reads	No. of Individuals	Ovine Weight, kg	Left Ventricle Weight, g
EFH	Heart muscle (left ventricle)	mRNA	1	>76 million paired-end reads per replica	3	1.43 ± 0.3	4.54 ± 0.9
LFH	Heart muscle (left ventricle)	mRNA	1	>59 million paired-end reads per replica	3	2.21 ± 0.6	6.55 ± 1.4
AH	Heart muscle (left ventricle)	mRNA	1	>73 million paired-end reads per replica	3	34.75 ± 4.1	93.44 ± 5.3

Values are means ± SE. AH, adult heart; EFH, early fetal heart; LFH, late fetal heart. The ovine weight and the left ventricle weight values correspond to the averaged weight of the 3 replicas in each experimental group.

AGCCTG-3′; reverse: 5′-AAGTCAGCGGGTCAATGGAG-3′), and *PCNA* (proliferating cell nuclear antigen; forward: 5′-GAGGGCTTC-GACACTTACCG-3′; reverse: 5′-TGCCAAGGTGTCCGCATTAT-3′) using the following thermal profile: 10′ at 95°C (1 cycle), 15′ at 95°C, and 1′ at 60°C (40 cycles). The constitutive *GAPDH* (glyceraldehyde-3-phosphate dehydrogenase; forward: 5′-TCTTCCAGGAGCGAGATCC-3′; reverse: 5′-TGAGCCCCAGCCTTCTCC-3′) RNA was used in each reaction as internal standard.

For each gene, a calibration curve was generated, and analysis was performed using the $2^{-\Delta\Delta C_T}$ method (29, 33, 58).

Histology. The hearts of each fetus ($n = 6$) and adult ($n = 3$) were excised, the atria and the right ventricle were removed, and the left ventricle was opened along the posterior interventricular sulcus. A myocardial sample measuring ~1 cm^2 was isolated and put in 4% formaldehyde at room temperature for 24 h. The fixed samples were next embedded in paraffin and cut into 4-μm sections. For immunohistochemistry, tissue sections were deparaffinized and brought to PBS solution (pH 7.2). Endogenous peroxidase was blocked with 3% H_2O_2 in methanol, antigens were retrieved with citrate buffer pretreatment in a microwave oven, and sections were incubated for 1 h with specific monoclonal antibodies according to published guidelines (5, 25) against PCNA (Biogenex, Fremont, CA) and against the cell cycle marker K_i-67 (Roche, Basel, Switzerland). Subsequently, sections were incubated with an anti-sarcomeric α-actin antibody (Sigma-Aldrich, St. Louis, MO). Biotin/streptavidin peroxidase was used as detection system and DAB chromogen as marker. All slices undergoing immunohistochemistry were counterstained with hematoxylin. Slides were analyzed under an optic microscope, and pictures were taken using a Micrometrics camera and software.

Statistical analysis. For intergroup comparisons, statistical analysis was performed using one-way ANOVA-Bonferroni. Results are expressed as means ± SD. For several analyses, the standard deviation was expressed as percentage of the mean for each TPMn (dispersion). Values of $P < 0.05$ were considered indicative of statistically significant differences (29).

RESULTS

RNA-seq data analysis. More than 59 million paired-end reads per RNA-seq's sample of ovine hearts that successfully passed the FastQC's analysis were obtained (Table 1). A transcript integrity analysis (TIN) was performed (Supplemental Fig. S1; available at https://doi.org/10.6084/m9.figshare.11764458).

With these data, a curated *Ovis Aries* reference transcriptome (containing 44,786 transcripts) and Salmon pipeline (47), the expression values in TPMs (transcripts per million), were determined for each protein-encoding gene, and then they were normalized with respect to TPM value of GAPDH mRNA (TPMn) (Fig. 1).

To provide a general view of the results, non-normalized TPM data from each replica in each experimental group (EFH, LFH, and AH) were represented in a plot considering the transcript length (Fig. 2).

The different replicas of each experimental group showed a similar pattern containing transcripts with effective length ranging from 128 to 16,384 nucleotides ($\log_2$ 7–14). An exception was Titin (TTN) and its transcriptional variants that have an approximate length of 131,072 nucleotides. The protein Titin is a molecular marker found at higher concentrations in the heart and skeletal muscle when compared with other tissues and has an important role in the organization and development of the sarcomere (26). Titin, a huge protein (3 to 4 MDa), takes part in the generation of passive force during skeletal muscle stretching (31). This protein works by directly or indirectly contributing and modulating active tension. It was also reported that Titin conformational changes can regulate several myocyte intracellular signaling events such as changes in protein degradation or synthesis rates (30). For this reason, having detected the *Titin* transcript in all the samples is an appropriate control that they contain cardiac muscle.

The transcripts were classified in non-detected (OFF) and detected (ON) categories in each experimental group using the TPMn values (Fig. 3). The amount of genes that were classified as OFF in the two fetal stages was similar, in contrast to AH, which showed 22% more turned-off genes with respect to the reference transcriptome.

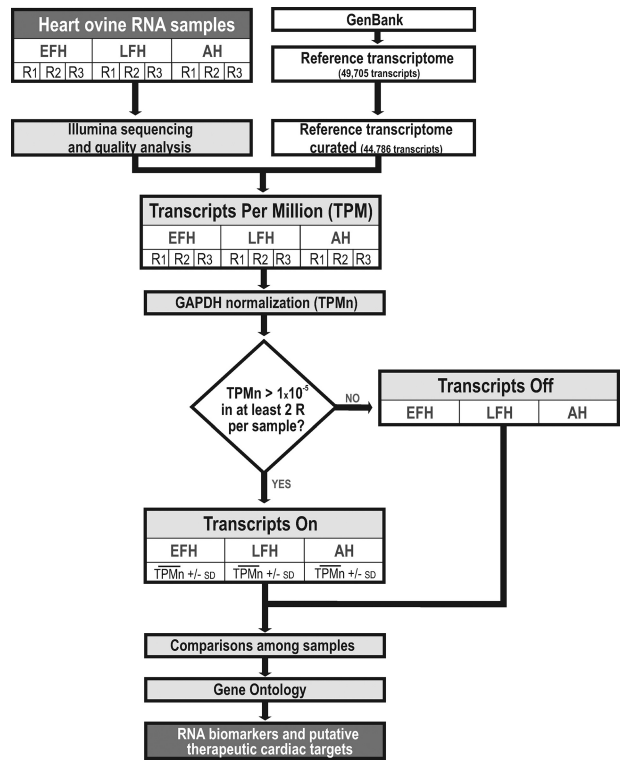

Fig. 1. Chart summarizing the analysis performed using RNAseq data from ovine hearts. AH, adult heart ($n = 3$; 2 males and 1 female); EFH, early fetal heart ($n = 3$; all male); LFH, late fetal heart ($n = 3$; all female); R, replica; TPMn, normalized TPM with GAPDH mRNA level.

Downloaded from journals.physiology.org/journal/ajpheart (168.096.240.002) on May 3, 2021.

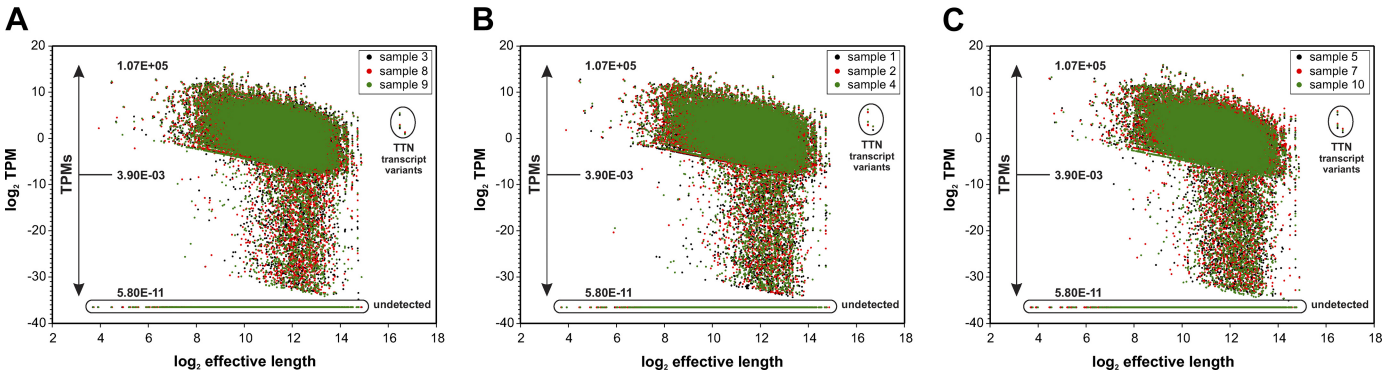

Fig. 2. Correlation between transcripts per million (TPM) abundance and transcript length. *A*: early fetal heart (EFH; $n = 3$, all males). *B*: late fetal heart (LFH; $n = 3$, all females). *C*: adult heart (AH; $n = 3$, 2 males and 1 female). Replicas of each experimental group are shown in different colors. The highlighted black circles show the 5 variants of Titin (TTN) gene. Only to make this plot clearer, transcripts with a TPM equal to zero were arbitrarily assigned to the value $1E^{-11}$.

Although the sheep taking part in this experiment belonged to the same breed, the genetic homogeneity is not as high as in a laboratory rodent. However, the 83–85% of the genes classified as ON was detected in the three replicas of each experimental group.

Additionally, a global analysis of TPMn dispersion values was carried out (Fig. 4*A*). The analysis revealed that most of the averaged TPMns show dispersion values of less than 20%. Besides, when analyzing the expression levels of five *Titin* transcriptional variants, it was observed that the three experimental groups showed similar values (Fig. 4*B*). These results strongly suggest that the three replicas of the different gestational ages are comparable and that they have the same general pattern than the global transcriptome, thus containing the same type of data with both similar characteristics and information.

Analysis of differential expression. Most of the transcripts classified as ON are shared in the three experimental groups (Fig. 5*A*). Particularly in EFH and LFH, 79% of the transcripts (21,585 of 27,196 and 27,258, respectively) are shared in the three stages, whereas in the AH 92% of the genes (21,585 of 23,377) are expressed in the other stages. Most of the 21,585 shared transcripts consistently showed low dispersion values (Supplemental Fig. S2; available at https://doi.org/10.6084/m9.figshare.9992267).

Moreover, this analysis revealed sets of genes exclusively expressed in a particular experimental group, turning them into "putative RNA biomarkers for these development timepoints." Thus, in the EFH, 6% of the transcripts (1,641) were unique, whereas in the LFH they were 5.5% (1,506), and in the AH only 2.8% (655) of the transcripts were exclusively expressed (Supplemental Table S1; available at https://doi.org/10.6084/m9.figshare.9992216).

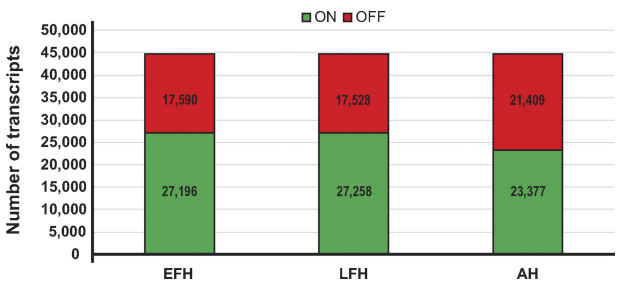

Fig. 3. Presence (ON)/absence (OFF) of *Ovis aries* transcripts in the 3 experimental groups. AH, adult heart ($n = 3$, 2 males and 1 female); EFH, early fetal heart ($n = 3$, all males); LFH, late fetal heart ($n = 3$, all females).

The transcripts that were detected in only one of the experimental groups could be considered a signature of that development time point (EFH, LFH, AH) for the analyzed samples (sheep cardiac left ventricle). Although validation in a larger number of animals (and its subsequent correlation with equivalent samples in other animal models and in humans) is needed, these lists of filtered genes help to narrow down the search for encoding sequences exclusively expressed in certain physiological conditions of large mammalian hearts. Moreover, proposing biomarkers that reflect physiological states of the heart can be useful to understand its biology and to diagnose potential pathological processes when the "signature" of transcripts does not coincide with that of a healthy physiological state.

Among transcripts shared by only two experimental groups, most of them were differentially expressed (87% of 3,500 transcripts between EFH and LFH, 91% of 667 transcripts between LFH and AH, and 92% of 470 between EFH and AH) (Fig. 5*A* and Supplemental Table S2; available at https://doi.org/10.6084/m9.figshare.9992213).

Among transcripts shared by the three experimental groups, there are 54% (11,703 of 21,585) that have similar levels of expression, but the rest of them show significantly different tendencies allowing for subclassifications, turning them into "RNA biomarkers of expression levels at certain developmental timepoints" (Fig. 5*B* and Supplemental Table S3; available at https://doi.org/10.6084/m9.figshare.9992219). After a thorough analysis, the seven subsets were characterized according to expression level pattern among the three experimental groups (EFH = LFH = AH, EFH > LFH > AH, EFH < LFH < AH, EFH = LFH > AH, and EFH = LFH < AH; Fig. 6).

This study also identified whether OFF transcripts were the same or unique for each experimental group (Fig. 5*C* and Supplemental Table S4; available at https://doi.org/10.6084/m9.figshare.9992225).

GO term enrichment analysis. GO analysis revealed that genes uniquely expressed in one of the three experimental groups or differentially expressed among stages were associated mainly with cellular processes (GO:0009987) and metabolic processes (GO:0008152). (Fig. 7, *A* and *C*).

Downloaded from journals.physiology.org/journal/ajpheart (168.096.240.002) on May 3, 2021.

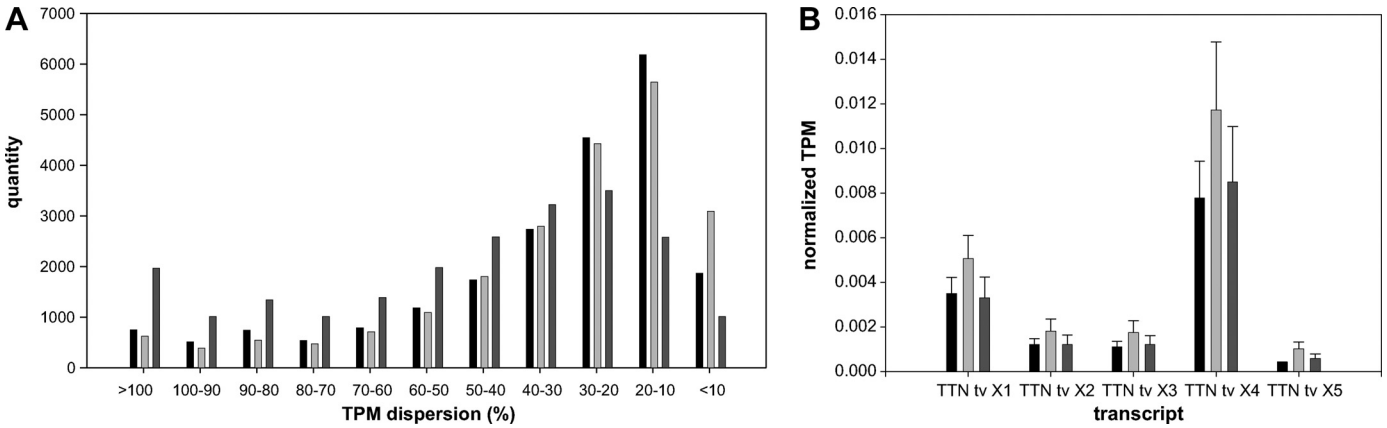

Fig. 4. Distribution of normalized transcripts per million with GAPDH mRNA level (TPMn) dispersion. In the 2 histograms, black, light gray, and dark gray bars correspond to early fetal heart (EFH; $n = 3$, all males), late fetal heart (LFH; $n = 3$, all females), and adult heart (AH; $n = 3$, 2 males and 1 female), respectively. *A*: global distribution of standard deviation expressed as %mean for each TPMn. *B*: expression levels of the 5 transcriptional variants (tv; the 5 variants are listed as X1, X2, X3, X4, and X5) of Titin (TTN) gene. Standard deviation is shown as error bars.

Inside the cellular processes classification it was possible to identify a subset of genes related to cell cycle (GO:0007049), corresponding to 9.6% in EFH and 12.4% in both LFH and AH (Fig. 7*B* and Supplemental Table S5; available at https://doi.org/10.6084/m9.figshare.9992222).

GO analysis was also performed for the set of transcripts classified as OFF. The genes in this classification for all of the combinations of experimental groups are mainly in the metabolic processes (GO:0008152) and biological regulation classifications (GO:0065007). (Fig. 7*D*).

Additionally, an analysis to evaluate the functional enrichment level of each GO term was carried out. For this, the biological process category and *Ovis aries* as species were selected and results expressed as heatmaps (Fig. 8 and Supplemental Fig. S3; available at https://doi.org/10.6084/m9.figshare.11764563). This analysis revealed the predominant expression of genes associated with cell division and development in fetal stages. Particularly, EFHs differentially express genes associated with cytokinesis (GO:0000910), cell division (GO:0051301), and mitotic chromosome condensation (GO:0007076), whereas LFHs differentially express genes related to post-embryonic development (GO:0009791), and both express genes linked to smooth muscle tissue development (GO:0048745), DNA replication (GO:0006260), and growth (GO:0040007) in similar levels.

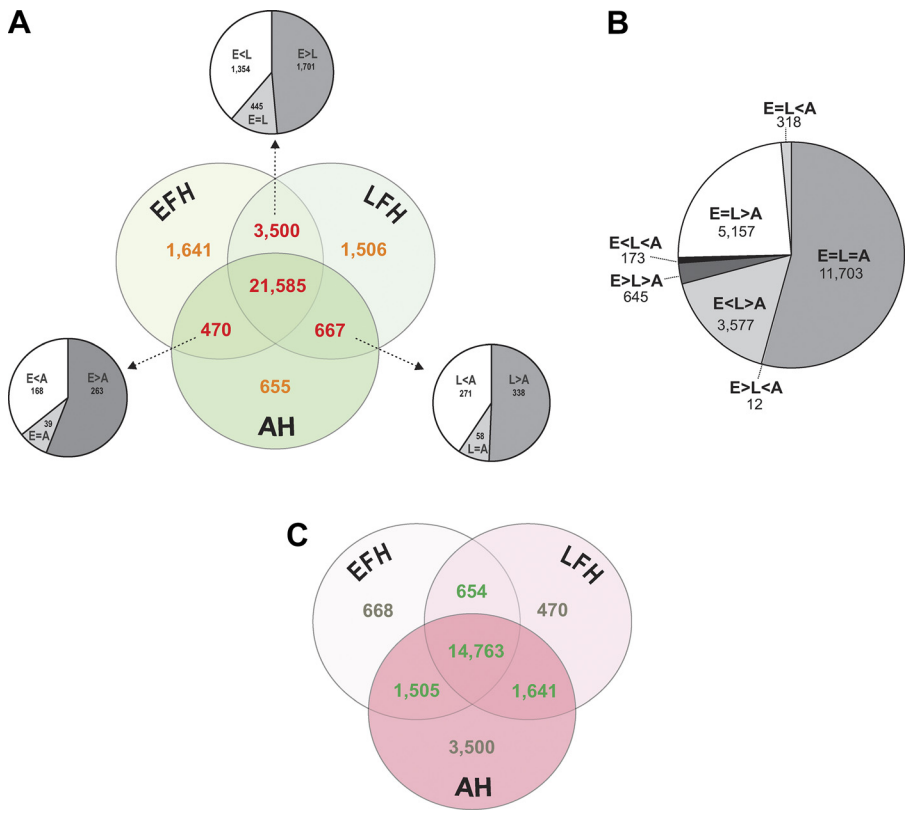

Fig. 5. Transcript subclassification according to ON/OFF status among experimental groups. *A*: Venn diagram showing the distribution of ON transcripts. Pie plots indicated with arrow show the distribution of transcripts shared by 2 experimental groups according to expression levels. *B*: pie plot showing the transcripts classified as ON in the 3 experimental groups, according to expression level variations. *C*: Venn diagram showing the distribution of the OFF transcripts. E = early fetal heart (EFH; $n = 3$, all males); L = late fetal heart (LFH; $n = 3$, all females); A = adult heart (AH; $n = 3$, 2 males and 1 female).

Downloaded from journals.physiology.org/journal/ajpheart (168.096.240.002) on May 3, 2021.

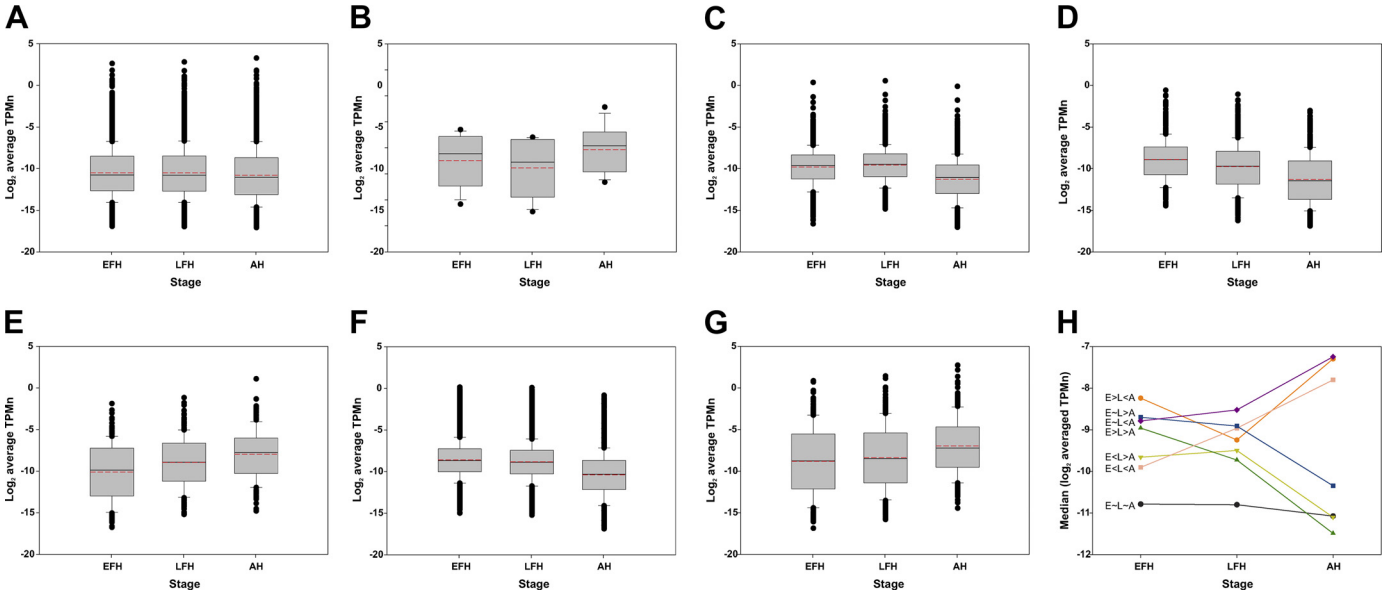

Fig. 6. Statistical analysis for shared differentially expressed genes. *A*–*G*: boxes contain the transcripts per million (TPMs) between percentiles 25 and 75. Values below or above these limits are shown as whiskers or outliers. Black solid line and the dashed red line indicate median and mean of TPMs, respectively. Box plots show the 7 classes of expression patterns among shared transcripts. *A*: early fetal heart (EFH) ~late fetal heart (LFH) ~adult heart (AH). *B*: EFH > LFH < AH. *C*: EFH < LFH > AH. *D*: EFH > LFH > AH. *E*: EFH < LFH < AH. *F*: EFH~LFH > AH. *G*: EFH ~LFH < AH. *H*: line and scatter plots summarize the tendencies in expression level changes for each of the expression patterns analyzed. ANOVA-Bonferroni (significance: $P < 0.05$) was performed to classify genes. E = EFH ($n = 3$, all males); L = LFH ($n = 3$, all females); A = AH ($n = 3$, 2 males and 1 female).

Evaluation of gene expression by RT-qPCR and histology. In view of the aim of this study, a group of genes profusely associated with cell cycle regulation were selected and their expression levels quantified by RT-qPCR employing the same total RNA used for the RNAseq (Fig. 9). The genes included *cyclin A*, *cdk2*, *meis2*, *meis3*, *meis1*, *p16* (*cdkn2aip*), *sav1*, *nkx2.5*, and *PCNA*. The results showed that through both methods there was a similar tendency in expression variation for all the analyzed genes when compared with the global RNAseq assay.

Particularly, the genes with a proposed function as cell cycle-positive regulators [*cyclin A*, *cdk2*, *meis2*, *meis3*, and *PCNA* (59, 61, 62, 74)] showed a higher expression level in fetal hearts and a lower expression in AH. Unexpectedly, genes proposed as cell cycle inhibitors [*meis1*, *p16*, and *sav1* (20, 37)], all of which showed consistent expression levels with both methods, tended to be higher in fetal than in adult hearts. It is important to note that although cell cycle promoters are almost not detectable in the AH, when analyzing the inhibitors there is a considerable level of expression in the same stage. These results suggest that the genes proposed as inhibitors are involved in several other cell processes, and not only cell cycle regulation and/or their biological role vary among different animal species.

Taking into account that cellular metabolic pathways change during development (12), a set of key genes was also studied by RT-qPCR (*ldhb*, *aldolase*, *enolase*, *ppargc1a*, *pitx*, and *adipoq*). Results showed a tendency similar to RNAseq assessment, highlighting the upregulation observed in fetal stages for *pitx* and *adipoq* genes (Fig. 10).

The histological analysis of EFH, LFH, and AH slides showed that the positive cell cycle regulator PCNA is present at higher levels in EFH (110 ± 48 positive nuclei/mm^2) with respect to LFH (43 ± 37 positive nuclei/mm^2, $P < 0.05$), while no PCNA was detected in AH tissues, consistently with the cell cycle marker K_i-67 in cardiomyocytes (EFH: 196 ± 68 positive nuclei/mm^2, LFH: 96 ± 39 positive nuclei/mm^2, and AH: 2 ± 1 positive nuclei/mm^2, $P < 0,5$) (Supplemental Fig. S4; available at https://doi.org/10.6084/m9.figshare.11764695).

DISCUSSION

The expression of genetic information toward proteins, the players that direct biological functions in cells, can be interpreted through the study of actively synthesized transcripts from different physiological/pathological situations. It is known that during heart development significant changes occur in different aspects such as growth, cell proliferation, function, and other metabolic characteristics. Accordingly, in this study the transcriptome profiles (RNAseq) of the sheep heart were characterized in three stages: adult (non-proliferative differentiated CMs) and fetus of two gestational ages (both proliferative CMs in process of differentiation) (28). This comparative transcriptomic analysis can provide information on varying levels of expression of specific transcripts that, in turn, can be used as possible targets in cardiac regeneration strategies.

RNAseq is a widely employed technique because it is highly informative, quantitative, and reproducible (29, 44, 70, 81), as it has been previously reported in sheep and other animal species (6). The assessment of data from transcriptomic analysis focused on proliferation and cell cycle regulators specifically in CMs should derive from the processing and disruption of whole cardiac tissue and CM isolation. However, as it is methodologically complex to separate CMs from the rest of the cells conforming the cardiac tissue without altering the expression profile, most published studies (3, 77, 80) either provide information resulting from the expression analysis of mRNA from whole heart or separate CMs following enzymatic protocols that take

Downloaded from journals.physiology.org/journal/ajpheart (168.096.240.002) on May 3, 2021.

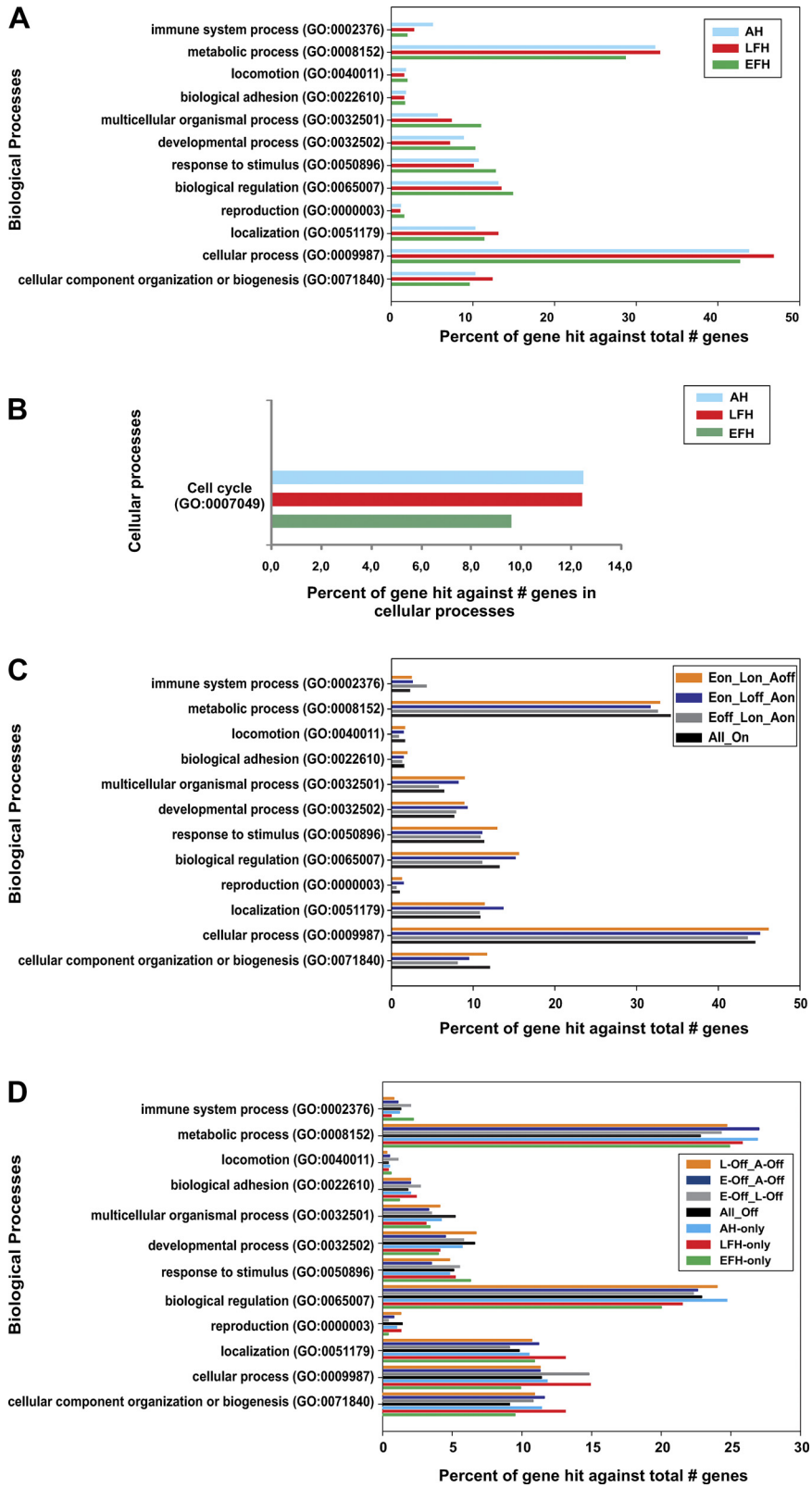

Fig. 7. Gene Ontology (GO) analysis. GO terms with adjusted P values of <0.05 and including at least 2 differentially expressed genes were considered for the 12 overrepresented biological processes. *A*: uniquely expressed genes for each experimental group [early fetal heart (EFH), late fetal heart (LFH), and adult heart (AH)]. *B*: subset of transcripts of cellular processes (GO:0009987) uniquely expressed in each experimental group related to cell cycle (GO:0007049). *C*: transcripts shared by 2 or 3 experimental groups (EFH-LFH-AH, LFH-AH, EFH-AH, EFH-LFH). *D*: non-detected transcripts in 1, 2, or 3 experimental groups (LFH-AH, EFH-AH, EFH-LFH, EFH-LFH-AH, AH, LFH, EFH). E = EFH (n = 3, all males); L = LFH (n = 3, all females); A = AH (n = 3, 2 males and 1 female).

several steps of tissue desegregation, at the risk of affecting and modifying the mRNA pool of the cells (83). It is important to take into account that the samples employed in this study come from an isolated portion of sheep hearts, so the variations in gene expression can come from physiological changes along development of the cells that conform the tissue, but they can also be caused by physiological changes in the diversity and proportion of cells in the sample. Taking these facts and limitations into ac-

Downloaded from journals.physiology.org/journal/ajpheart (168.096.240.002) on May 3, 2021.

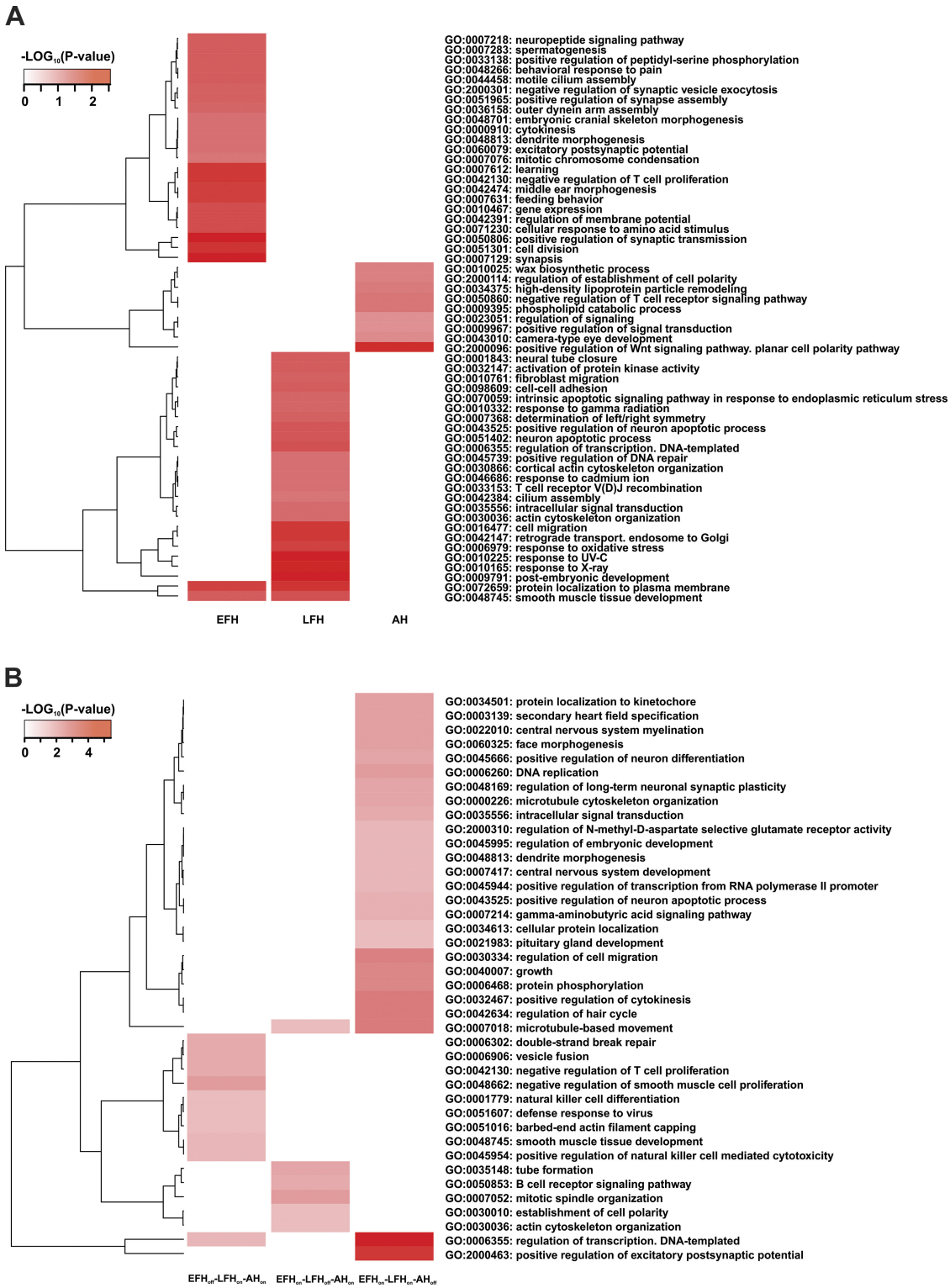

Fig. 8. Clustered heat map of enriched Gene Ontology (GO) terms in the biological process category. GO terms associated with genes expressed only in 1 stage, early fetal heart (EFH; $n = 3$, all males), late fetal heart (LFH; $n = 3$, all females), and adult heart (AH; $n = 3$, 2 males and 1 female) (*A*) and in 2 of the 3 stages, EFH_{off}-LFH_{on}-AH_{on} (transcripts expressed in LFH and AH), EFH_{on}-LFH_{off}-AH_{on} (transcripts expressed in EFH and AH), and EFH_{on}-LFH_{on}-AH_{off} (transcripts expressed in EFH and LFH) (*B*). Color scale indicates the level of enrichment score [$-LOG_{10}$ (*P* value)] of GO terms. Red, high significance; white, low significance.

Downloaded from journals.physiology.org/journal/ajpheart (168.096.240.002) on May 3, 2021.

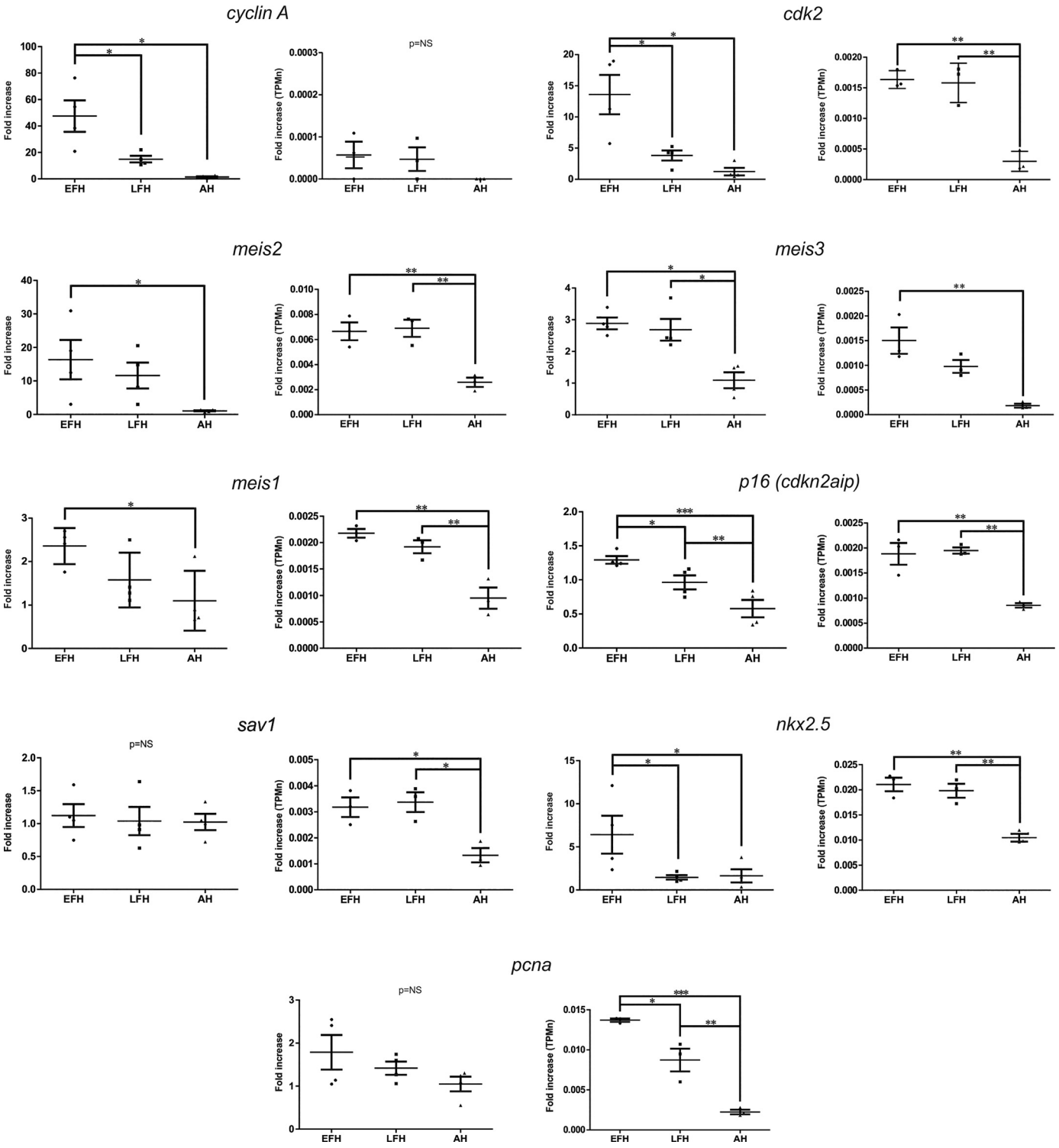

Fig. 9. Quantification of cell cycle gene expression by RT-quantitative (q)PCR. The dot/whisker plots on the *left* correspond to the qPCR analysis ($2^{-\Delta\Delta Ct}$) and the ones on the *right* to RNA-seq quantification [normalized transcripts per million with GAPDH mRNA level (TPMn)]. Each transcript is indicated above the histogram. AH, adult heart ($n = 4$ for qPCR, 2 males and 2 females; and $n = 3$ for RNAseq, 2 males and 1 female); EFH, early fetal heart ($n = 4$ for qPCR and $n = 3$ for RNAseq, all males); LFH, late fetal heart ($n = 4$ for qPCR and $n = 3$ for RNA-seq, all females). Error bars: standard deviation. P = not significant (NS). *$P < 0.05$; **$P < 0.01$; ***$P < 0.001$.

count, in this study the whole cardiac tissue was employed to provide the analysis of the heart trancriptomes.

Mammalian organs are made up of different cell types that act in coordination to support physiological functions. In some way, each organ can be considered as an ecosystem that, due to transient or chronic alterations in environmental conditions or in its components (new invading cells of the same organism or their own cell types that increase their proportion in detriment

Downloaded from journals.physiology.org/journal/ajpheart (168.096.240.002) on May 3, 2021.

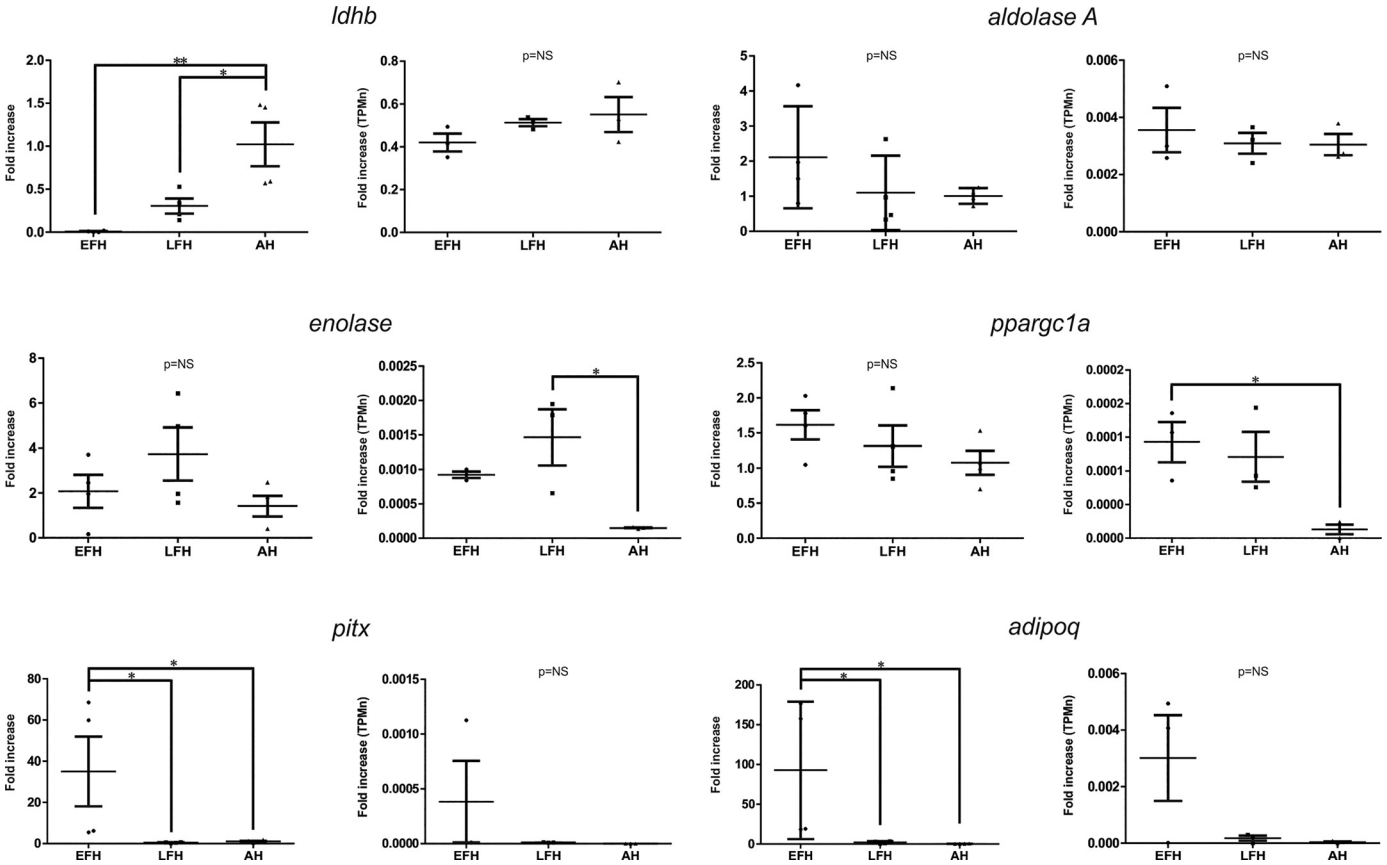

Fig. 10. Quantification of metabolic process gene expression by RT-quantitative (q)PCR. The dot/whisker plots on the *left* correspond to the qPCR analysis ($2^{-\Delta\Delta C_T}$) and the ones on the *right* to RNA-seq quantification [normalized transcripts per million with GAPDH mRNA level (TPMn)]. Each transcript is indicated above the histogram. AH, adult heart ($n = 4$ for qPCR, 2 males and 2 females and $n = 3$ for RNAseq, 2 males and 1 female); EFH, early fetal heart ($n = 4$ for qPCR and $n = 3$ for RNA-seq, all males); LFH, late fetal heart ($n = 4$ for qPCR and $n = 3$ for RNAseq, all females). Error bars: standard deviation. P = not significant (NS). *$P < 0.05$; **$P < 0.01$.

of others), can lead to pathological states that, over time, impact on the entire body. Because gene transcription analysis is an important tool to evaluate organic functions and the dynamics of biological responses to diverse situations and stresses (age and development, circadian cycle, hormonal influence, inflammation, ischemia, infections, oncological processes, etc.), experimental studies enabling global RNAseq-based analyses of transcripts derived from a biomass have become a central tool in life sciences (40).

Currently, there is debate on whether the biomass to be interrogated should be a portion of the organ (bulk RNAseq) (80), each cell type separately (single-cell RNAseq) (39, 52, 73), or the nuclei of each cell type (single-nucleus RNAseq) (13, 22, 24). The individual study of each of the cell populations that build a complex organ can provide a greater degree of precision in the analysis of the dynamics of gene expression and cell diversity and specialization. However, as previously mentioned, the methodological procedures that allow the deconstruction of a biomass in its component cells usually take a long time and are not always completely possible (some cells of an organ are more dissociable than others), and, most importantly, they can result in stresses that change and skew the type and relative number of transcripts detected (67). On the other hand, single-nucleus RNAseq approaches, although partially able to circumvent the problem mentioned above, reduce the available information to only what is in the cell nucleus. Therefore, the bulk RNAseq applied on an organ in different conditions (in the present study, different stages of heart development) is a suitable initial experimental approach to explore differential gene expression because it contains all RNAs present in the biomass (both nuclear and cytoplasmatic) without bias attributable to laboratory stressors. This approach resembles a meta-transcriptomic study such as that performed in environmental samples where the emergence of biological properties is a cause of their biological diversity and cross talk (2). Thus, the type of analysis used in the present study provides a good initial picture of the mammalian heart development, highlighting the importance of some genes decisive for activating (fetal stages) or arresting (adult stage) the cardiomyocyte cell cycle, which can then be studied in greater depth by the other RNAseq approaches mentioned, as well as by traditional molecular methods of individual monitoring.

Regarding the animal model employed, in large mammals such as sheep, usually used as farm animals, there are considerable differences among individuals even of the same breed, unlike laboratory rodents, which show important similarities in genetic background. This fact may affect the robustness of the biological data derived from different experimental replicas. However, the results derived from replicas in this study show

Downloaded from journals.physiology.org/journal/ajpheart (168.096.240.002) on May 3, 2021.

a high consistency on account of very low dispersion observed among them for each detected gene.

This study provides a classification of transcripts, allowing for the discovery of sets of genes that are uniquely expressed in specific time points of ovine heart development, and which constitute putative RNA biomarkers of these development time points.

By the use of the gene ontology analysis, it was possible to select groups of transcripts associated to cell cycle regulation. Several transcripts were found only in EFH, including *cdca3* (cell division cycle-associated protein 3), a gene proposed as a mediator of the ubiquitination and degradation of WEE1 kinase at G2/M phase (1); *myog* (myogenin), proposed as a transcriptional activator of muscle-specific target genes collaborating in cell differentiation (19); *mapre2* (microtubule-associated protein RP/EB family member 2), presumably involved in microtubule dynamics associated with centrosomes (68); and *lin54* (protein lin-54 homolog), encoding a protein that forms a complex that activates or represses the cell cycle, modulating hundreds of genes (32,57). Other transcripts were exclusively found in LFH, such as *cdk20* (cyclin-dependent kinase 20), a CDK2 activator (61); *cinp* (cyclin-dependent kinase 2-interacting protein), proposed to have an important role as cyclin activator (14); *fign* (fidgetin), regulating microtubule dynamics from the mitotic spindles (45); *usp9x* (probable ubiquitin carboxyl-terminal hydrolase FAF-X), which regulates the chromosome segregation and alignment in mitosis, its expression being associated with undifferentiated cells (46); and *ks6a3* (ribosomal protein S6 kinase α-3), an inhibitor of G1 phase progression (8). Finally, some transcripts were expressed only in the AH, such as *rad17* (cell cycle checkpoint protein RAD17), which plays a role in the maintenance of chromosomal stability (among other functions) (51), and *q8ndn9* (RCC1 and BTB domain-containing protein 1), which is linked to chromatin remodeling (36). It is important to note that many of the transcripts exclusively expressed in each of the three experimental groups still lack an identity and a proposed function, making it possible to find among them several other transcripts with an important role in cell cycle.

Gene ontology analysis was also performed for the transcripts shared in the three experimental groups but having significant variation in expression levels among them. Especially interesting is the group of transcripts that were enriched in fetal stages because they might be associated with cell proliferation pathways. One of these transcripts is *fam64a* (family with sequence similarity 64 member A isoform 1). This gene was recently proposed as a relevant cell cycle regulator in hypoxic fetal cardiomyocytes in mice (18). These authors found that the protein Fam64a had a nuclear location and that its expression level dramatically decreased by oxygen exposure in cell culture and in neonatal cardioyocytes after birth following the first breath. Interestingly, the sheep heart showed the same pattern in Fam64a expression, with a high expression level in EFH and a statistically significant decrease in LFH and AH (100-fold increase in fetal versus adult heart). These results highlight Fam64a as a key regulator of cardiomyocyte cell cycle in mammals. Additionally, recent evidence showed that Fam64a overexpressed in cancer cells was associated with poor prognosis (72, 82). Another differentially expressed gene (DEG) is *CDC20* (cell division cycle protein 20 homolog), which was enriched in fetal hearts with respect to adult hearts (~50-fold). This gene is an activator of the anaphase-promoting complex (APC) (16, 76) and an essential developmental gene whose inhibition in mice causes embryonic lethality through massive cell cycle arrest (27). In a similar way, a very important regulator of cell cycle, *CDK1* (cyclin-dependent kinase 1), showed the highest expression level in fetal hearts (~80-fold) (42).

In contrast, most of the DEGs overexpressed in adult hearts were associated with structural proteins present in differentiated cardiomyocytes. For example, the sarcomeric proteins encoded by the genes TPM3 (tropomyosin α-3 chain) and MYOM3 (myomesin-3) (71) and the proteins related to fatty acid metabolism, such as cardiac-specific PDK4 (pyruvate dehydrogenase kinase isozyme 4), showed a fold increase of around 100, 50, and 30, respectively (7,56).

With regard to genes associated with metabolic processes, it is interesting to observe that *pitx* (expression pattern EFH_{on}-$LFH_{on}AH_{off}$) and *adipoq* (~1,000-fold increase EFH versus AH), which have been shown very recently to be linked to ischemic injury protection (17,85) and even to cardiac regeneration (64), were highly expressed in EFH and undetectable in AH. Specifically, *pitx2c* was found to be downregulated in the postnatal pig heart (66), in accordance with the findings in sheep provided by this study.

Several studies have employed RNAseq in heart tissue from different mammals. Some cardiac embryonic transcription factors such as *nkx 2.5* (nk2 homeobox 5), aurora B kinase, *tbx5* (T-box transcription factor 5), and *gata6* (transcription factor gata-6), considered early markers of myocardial progenitor cells in humans (10), pigs (78), and mice (48), displayed the same pattern in the present study, showing upregulation in EFH. Besides, it has been reported that non-CM cells highly express *hapln1* (hyaluronan and proteoglycan link protein 1), *hmga1* (high-mobility group AT-hook protein), and *fabp4* (fatty acid-binding protein 4) genes, which are associated with developmental extracellular matrix interactions, chromatin organization, and metabolic shift from glycolysis to oxidative phosphorylation, respectively (9). Coincidently, sheep hearts in this study showed upregulated levels of these genes in EFH. Moreover, the co-activators *MRT-F*, *A* and *B* (myocardin-related transcription factors A and B), of the serum response factor (SRF), which is an essential transcription factor for cardiac development, were highly expressed in sheep EFH, as previously reported in mouse (43).

The same occurred with *mbnl1* (muscleblind-like splicing regulator 1), *rbfox2* (RNA-binding protein fox-2), and *adar1* (RNA-specific adenosine deaminase 1) genes, which express RNA splicing and editing proteins in fetal hearts and decrease in postnatal life (11).

By contrast, some specific marker genes of cardiomycocyte differentiation in mouse hearts as *myh7* (myosin heavy chain 7), *tnnt2* (cardiac troponin T2), *tnnc1* (cardiac troponin C1), *tnni3* (cardiac troponin I3), and *myl3* (myosin light chain 3) (9) were all detected in sheep's AH. In agreement with an atlas of circadian-expressed genes in different adult mouse organs, including the heart (84), in adult sheep *kdr* (kinase insert domain receptor) and *vegfa* (vascular endothelial growth factor A) genes were downregulated, whereas *flt1* (fms-related receptor tyrosine kinase 1) was upregulated.

Other reports showed several markers of the differentiation trajectory in human cardiomyocytes derived from embryonic

Downloaded from journals.physiology.org/journal/ajpheart (168.096.240.002) on May 3, 2021.

stem cells, such as *sox17* (sry-box transcription factor 17; a mesoderm induction marker), *mef2c* (myocyte enhancer factor 2c; a committed cardiomyocyte marker), and *tnni3* (a mature cardiomyocyte marker) (55). In the present study, these genes were consistently upregulated in EFH, LFH, and AH, respectively, supporting the appropriateness of the development stages selected.

Conclusion. This study provides sets of transcripts whose variation in expression level or exclusive detection in only one of the ovine heart developmental stages may link them to a specific role in cell cycle regulation. The transcriptomic profile in fetal hearts revealed that several transcripts overexpressed or uniquely expressed at this time point are associated with cell cycle promotion; indeed, some of them are related to uncontrolled cell proliferation in cancer. By contrast, transcripts expressed in adult hearts are associated mainly with its physiological functions, suggesting that cell cycle arrest may be regulated by epigenetic mechanisms and posttranscriptional gene silencing as well.

From a translational point of view, this study shows several cell cycle-promoting genes that can be assessed in further cardiac tissue regeneration protocols. To our knowledge, this is the first time that an RNAseq analysis has been carried out in sheep heart tissue to compare different stages of fetal heart development with a focus on cell cycle regulation.

ACKNOWLEDGMENTS

We thank veterinarians María Inés Besansón and Pedro Iguain for anesthetic management and animal house assistants Juan Carlos Mansilla, Osvaldo Sosa, and Juan Ocampo for dedicated care of the animals. We also thank Julio Martínez and Fabián Gauna for technical help and Araceli Castro for her assistance in performing immunohistochemistry.

GRANTS

This project was supported by Grant 2015-2586 from the National Agency for the Promotion of Science and Technology (ANPCyT) and the Ministry of Science, Technology and Innovative Production (MINCyT) of Argentina.

DISCLAIMERS

The funding agencies had no role in the study design, data collection and analysis, decision to publish, or preparation of the manuscript.

DISCLOSURES

No conflicts of interest, financial or otherwise, are declared by the authors.

AUTHOR CONTRIBUTIONS

P.L., M.N.B., and F.D.O. conceived and designed research; A.E.L., M.d.R.B., and P.D.G. performed experiments; M.N.B., M.U.V., C.S.G., C.S.C., and P.D.G. analyzed data; P.L., M.G.C., C.S.C., and P.D.G. interpreted results of experiments; M.N.B. and C.S.C. drafted manuscript; P.L., L.A.C., A.C., and P.D.G. edited and revised manuscript; A.E.L., A.S., and C.S.C. prepared figures; A.C. approved final version of manuscript.

REFERENCES

1. **Adams MN, Burgess JT, He Y, Gately K, Snell C, Zhang SD, Hooper JD, Richard DJ, O'Byrne KJ.** Expression of CDCA3 is a prognostic biomarker and potential therapeutic target in non-small cell lung cancer. *J Thorac Oncol* 12: 1071–1084, 2017. doi:10.1016/j.jtho.2017.04.018.
2. **Althani AA, Marei HE, Hamdi WS, Nasrallah GK, El Zowalaty ME, Al Khodor S, Al-Asmakh M, Abdel-Aziz H, Cenciarelli C.** Human Microbiome and its Association With Health and Diseases. *J Cell Physiol* 231: 1688–1694, 2016. doi:10.1002/jcp.25284.
3. **An CI, Ichihashi Y, Peng J, Sinha NR, Hagiwara N.** Transcriptome dynamics and potential roles of Sox6 in the postnatal heart. *PLoS One* 11: e0166574, 2016. doi:10.1371/journal.pone.0166574.
4. **Andrews S.** Data from FastQC: A quality control tool for high throughput sequence data (Online). http://www.bioinformatics.babraham.ac.uk?/projects/fastqc/. Cambridge, UK: Babraham Institute Bioinformatics [January 2019].
5. **Brooks HL, Lindsey ML.** Guidelines for authors and reviewers on antibody use in physiology studies. *Am J Physiol Heart Circ Physiol* 314: H724–H732, 2018. doi:10.1152/ajpheart.00512.2017.
6. **Clark EL, Bush SJ, McCulloch MEB, Farquhar IL, Young R, Lefevre L, Pridans C, Tsang HG, Wu C, Afrasiabi C, Watson M, Whitelaw CB, Freeman TC, Summers KM, Archibald AL, Hume DA.** A high resolution atlas of gene expression in the domestic sheep (Ovis aries). *PLoS Genet* 13: e1006997, 2017. doi:10.1371/journal.pgen.1006997.
7. **Crewe C, Kinter M, Szweda LI.** Rapid inhibition of pyruvate dehydrogenase: an initiating event in high dietary fat-induced loss of metabolic flexibility in the heart. *PLoS One* 8: e77280, 2013. doi:10.1371/journal.pone.0077280.
8. **De Cesare D, Jacquot S, Hanauer A, Sassone-Corsi P.** Rsk-2 activity is necessary for epidermal growth factor-induced phosphorylation of CREB protein and transcription of c-fos gene. *Proc Natl Acad Sci USA* 95: 12202–12207, 1998. doi:10.1073/pnas.95.21.12202.
9. **DeLaughter DM, Bick AG, Wakimoto H, McKean D, Gorham JM, Kathiriya IS, Hinson JT, Homsy J, Gray J, Pu W, Bruneau BG, Seidman JG, Seidman CE.** Single-Cell Resolution of Temporal Gene Expression during Heart Development. *Dev Cell* 39: 480–490, 2016. doi:10.1016/j.devcel.2016.10.001.
10. **Elliott DA, Braam SR, Koutsis K, Ng ES, Jenny R, Lagerqvist EL, Biben C, Hatzistavrou T, Hirst CE, Yu QC, Skelton RJ, Ward-van Oostwaard D, Lim SM, Khammy O, Li X, Hawes SM, Davis RP, Goulburn AL, Passier R, Prall OW, Haynes JM, Pouton CW, Kaye DM, Mummery CL, Elefanty AG, Stanley EG.** NKX2-5(eGFP/w) hESCs for isolation of human cardiac progenitors and cardiomyocytes. *Nat Methods* 8: 1037–1040, 2011. doi:10.1038/nmeth.1740.
11. **Gao C, Wang Y.** Transcriptome complexity in cardiac development and diseases–an expanding universe between genome and phenome. *Circ J* 78: 1038–1047, 2014. doi:10.1253/circj.CJ-14-0412.
12. **Gibb AA, Hill BG.** Metabolic Coordination of Physiological and Pathological Cardiac Remodeling. *Circ Res* 123: 107–128, 2018. doi:10.1161/CIRCRESAHA.118.312017.
13. **Grindberg RV, Yee-Greenbaum JL, McConnell MJ, Novotny M, O'Shaughnessy AL, Lambert GM, Araúzo-Bravo MJ, Lee J, Fishman M, Robbins GE, Lin X, Venepally P, Badger JH, Galbraith DW, Gage FH, Lasken RS.** RNA-sequencing from single nuclei. *Proc Natl Acad Sci USA* 110: 19802–19807, 2013. doi:10.1073/pnas.1319700110.
14. **Grishina I, Lattes B.** A novel Cdk2 interactor is phosphorylated by Cdc7 and associates with components of the replication complexes. *Cell Cycle* 4: 4120–4126, 2005. doi:10.4161/cc.4.8.1918.
16. **Hadjihannas MV, Bernkopf DB, Brückner M, Behrens J.** Cell cycle control of Wnt/β-catenin signalling by conductin/axin2 through CDC20. *EMBO Rep* 13: 347–354, 2012. doi:10.1038/embor.2012.12.
17. **Hao R, Su G, Sun X, Kong X, Zhu C, Su G.** Adiponectin attenuates lipopolysaccharide-induced cell injury of H9c2 cells by regulating AMPK pathway. *Acta Biochim Biophys Sin (Shanghai)* 51: 168–177, 2019. doi:10.1093/abbs/gmy162.
18. **Hashimoto K, Kodama A, Honda T, Hanashima A, Ujihara Y, Murayama T, Nishimatsu SI, Mohri S.** Fam64a is a novel cell cycle promoter of hypoxic fetal cardiomyocytes in mice. *Sci Rep* 7: 4486, 2017. doi:10.1038/s41598-017-04823-1.
19. **Hasty P, Bradley A, Morris JH, Edmondson DG, Venuti JM, Olson EN, Klein WH.** Muscle deficiency and neonatal death in mice with a targeted mutation in the myogenin gene. *Nature* 364: 501–506, 1993. doi:10.1038/364501a0.
20. **Heallen T, Morikawa Y, Leach J, Tao G, Willerson JT, Johnson RL, Martin JF.** Hippo signaling impedes adult heart regeneration. *Development* 140: 4683–4690, 2013. doi:10.1242/dev.102798.
21. **Hnatiuk AP, Ong SG, Olea FD, Locatelli P, Riegler J, Lee WH, Jen CH, De Lorenzi A, Giménez CS, Laguens R, Wu JC, Crottogini A.** Allogeneic mesenchymal stromal cells overexpressing mutant human hypoxia-inducible factor 1-α (HIF1-α) in an ovine model of acute myocardial infarction. *J Am Heart Assoc* 5: e003714, 2016. doi:10.1161/JAHA.116.003714.
22. **Hu P, Liu J, Zhao J, Wilkins BJ, Lupino K, Wu H, Pei L.** Single-nucleus transcriptomic survey of cell diversity and functional maturation in postnatal mammalian hearts. *Genes Dev* 32: 1344–1357, 2018. doi:10.1101/gad.316802.118.

Downloaded from journals.physiology.org/journal/ajpheart (168.096.240.002) on May 3, 2021.

23. **Katz MG, Fargnoli AS, Kendle AP, Hajjar RJ, Bridges CR.** The role of microRNAs in cardiac development and regenerative capacity. *Am J Physiol Heart Circ Physiol* 310: H528–H541, 2016. doi:10.1152/ajpheart.00181.2015.
24. **Lake BB, Ai R, Kaeser GE, Salathia NS, Yung YC, Liu R, Wildberg A, Gao D, Fung HL, Chen S, Vijayaraghavan R, Wong J, Chen A, Sheng X, Kaper F, Shen R, Ronaghi M, Fan JB, Wang W, Chun J, Zhang K.** Neuronal subtypes and diversity revealed by single-nucleus RNA sequencing of the human brain. *Science* 352: 1586–1590, 2016. doi:10.1126/science.aaf1204.
25. **Leone M, Magadum A, Engel FB.** Cardiomyocyte proliferation in cardiac development and regeneration: a guide to methodologies and interpretations. *Am J Physiol Heart Circ Physiol* 309: H1237–H1250, 2015. doi:10.1152/ajpheart.00559.2015.
26. **LeWinter MM, Granzier H.** Cardiac titin: a multifunctional giant. *Circulation* 121: 2137–2145, 2010. doi:10.1161/CIRCULATIONAHA.109.860171.
27. **Li M, York JP, Zhang P.** Loss of Cdc20 causes a securin-dependent metaphase arrest in two-cell mouse embryos. *Mol Cell Biol* 27: 3481–3488, 2007. doi:10.1128/MCB.02088-06.
28. **Lindgren IM, Drake RR, Chattergoon NN, Thornburg KL.** Down-regulation of MEIS1 promotes the maturation of oxidative phosphorylation in perinatal cardiomyocytes. *FASEB J* 33: 7417–7426, 2019. doi:10.1096/fj.201801330RR.
29. **Lindsey ML, Gray GA, Wood SK, Curran-Everett D.** Statistical considerations in reporting cardiovascular research. *Am J Physiol Heart Circ Physiol* 315: H303–H313, 2018. doi:10.1152/ajpheart.00309.2018.
30. **Linke WA, Krüger M.** The giant protein titin as an integrator of myocyte signaling pathways. *Physiology (Bethesda)* 25: 186–198, 2010. doi:10.1152/physiol.00005.2010.
31. **Linke WA.** Titin gene and protein functions in passive and active muscle. *Annu Rev Physiol* 80: 389–411, 2018. doi:10.1146/annurev-physiol-021317-121234.
32. **Litovchick L, Sadasivam S, Florens L, Zhu X, Swanson SK, Velmurugan S, Chen R, Washburn MP, Liu XS, DeCaprio JA.** Evolutionarily conserved multisubunit RBL2/p130 and E2F4 protein complex represses human cell cycle-dependent genes in quiescence. *Mol Cell* 26: 539–551, 2007. doi:10.1016/j.molcel.2007.04.015.
33. **Livak KJ, Schmittgen TD.** Analysis of relative gene expression data using real-time quantitative PCR and the 2(−Delta Delta C(T)) Method. *Methods* 25: 402–408, 2001. doi:10.1006/meth.2001.1262.
34. **Locatelli P, Olea FD, Hnatiuk A, De Lorenzi A, Cerdá M, Giménez CS, Sepúlveda D, Laguens R, Crottogini A.** Mesenchymal stromal cells overexpressing vascular endothelial growth factor in ovine myocardial infarction. *Gene Ther* 22: 449–457, 2015. doi:10.1038/gt.2015.28.
35. **Locatelli P, Olea FD, Mendiz O, Salmo F, Fazzi L, Hnatiuk A, Laguens R, Crottogini A.** An ovine model of postinfarction dilated cardiomyopathy in animals with highly variable coronary anatomy. *ILAR J* 52: E16–E21, 2011. doi:10.1093/ilar.52.1.E16.
36. **Mabuchi H, Fujii H, Calin G, Alder H, Negrini M, Rassenti L, Kipps TJ, Bullrich F, Croce CM.** Cloning and characterization of CLLD6, CLLD7, and CLLD8, novel candidate genes for leukemogenesis at chromosome 13q14, a region commonly deleted in B-cell chronic lymphocytic leukemia. *Cancer Res* 61: 2870–2877, 2001.
37. **Mahmoud AI, Kocabas F, Muralidhar SA, Kimura W, Koura AS, Thet S, Porrello ER, Sadek HA.** Meis1 regulates postnatal cardiomyocyte cell cycle arrest. *Nature* 497: 249–253, 2013. doi:10.1038/nature12054.
38. **Makkar RR, Smith RR, Cheng K, Malliaras K, Thomson LE, Berman D, Czer LS, Marbán L, Mendizabal A, Johnston PV, Russell SD, Schuleri KH, Lardo AC, Gerstenblith G, Marbán E.** Intracoronary cardiosphere-derived cells for heart regeneration after myocardial infarction (CADUCEUS): a prospective, randomised phase 1 trial. *Lancet* 379: 895–904, 2012. doi:10.1016/S0140-6736(12)60195-0.
39. **Massaia A, Chaves P, Samari S, Miragaia RJ, Meyer K, Teichmann SA, Noseda M.** Single Cell Gene Expression to Understand the Dynamic Architecture of the Heart. *Front Cardiovasc Med* 5: 167, 2018. doi:10.3389/fcvm.2018.00167.
40. **Matkovich SJ.** Transcriptome analysis in heart failure. *Curr Opin Cardiol* 31: 242–248, 2016. doi:10.1097/HCO.0000000000000275.
41. **Mi H, Huang X, Muruganujan A, Tang H, Mills C, Kang D, Thomas PD.** PANTHER version 11: expanded annotation data from Gene Ontology and Reactome pathways, and data analysis tool enhancements. *Nucleic Acids Res* 45: D183–D189, 2017. doi:10.1093/nar/gkw1138.
42. **Miettinen TP, Kang JH, Yang LF, Manalis SR.** Mammalian cell growth dynamics in mitosis. *eLife* 8: e44700, 2019. doi:10.7554/eLife.44700.
43. **Mokalled MH, Carroll KJ, Cenik BK, Chen B, Liu N, Olson EN, Bassel-Duby R.** Myocardin-related transcription factors are required for cardiac development and function. *Dev Biol* 406: 109–116, 2015. doi:10.1016/j.ydbio.2015.09.006.
44. **Mortazavi A, Williams BA, McCue K, Schaeffer L, Wold B.** Mapping and quantifying mammalian transcriptomes by RNA-Seq. *Nat Methods* 5: 621–628, 2008. doi:10.1038/nmeth.1226.
45. **Mukherjee S, Diaz Valencia JD, Stewman S, Metz J, Monnier S, Rath U, Asenjo AB, Charafeddine RA, Sosa HJ, Ross JL, Ma A, Sharp DJ.** Human Fidgetin is a microtubule severing the enzyme and minus-end depolymerase that regulates mitosis. *Cell Cycle* 11: 2359–2366, 2012. doi:10.4161/cc.20849.
46. **Murtaza M, Jolly LA, Gecz J, Wood SA.** La FAM fatale: USP9X in development and disease. *Cell Mol Life Sci* 72: 2075–2089, 2015. doi:10.1007/s00018-015-1851-0.
47. **Patro R, Duggal G, Love MI, Irizarry RA, Kingsford C.** Salmon provides fast and bias-aware quantification of transcript expression. *Nat Methods* 14: 417–419, 2017. doi:10.1038/nmeth.4197.
48. **Pawlak M, Niescierowicz K, Winata CL.** Decoding the heart through next generation sequencing approaches. *Genes (Basel)* 9: 289, 2018. doi:10.3390/genes9060289.
49. **Porrello ER, Mahmoud AI, Simpson E, Hill JA, Richardson JA, Olson EN, Sadek HA.** Transient regenerative potential of the neonatal mouse heart. *Science* 331: 1078–1080, 2011. doi:10.1126/science.1200708.
50. **Porrello ER, Mahmoud AI, Simpson E, Johnson BA, Grinsfelder D, Canseco D, Mammen PP, Rothermel BA, Olson EN, Sadek HA.** Regulation of neonatal and adult mammalian heart regeneration by the miR-15 family. *Proc Natl Acad Sci USA* 110: 187–192, 2013. doi:10.1073/pnas.1208863110.
51. **Post SM, Tomkinson AE, Lee EY.** The human checkpoint Rad protein Rad17 is chromatin-associated throughout the cell cycle, localizes to DNA replication sites, and interacts with DNA polymerase ε. *Nucleic Acids Res* 31: 5568–5575, 2003. doi:10.1093/nar/gkg765.
52. **Quaife-Ryan GA, Sim CB, Ziemann M, Kaspi A, Rafehi H, Ramialison M, El-Osta A, Hudson JE, Porrello ER.** Multicellular Transcriptional Analysis of Mammalian Heart Regeneration. *Circulation* 136: 1123–1139, 2017. doi:10.1161/CIRCULATIONAHA.117.028252.
53. **Roncalli J, Mouquet F, Piot C, Trochu JN, Le Corvoisier P, Neuder Y, Le Tourneau T, Agostini D, Gaxotte V, Sportouch C, Galinier M, Crochet D, Teiger E, Richard MJ, Polge AS, Beregi JP, Manrique A, Carrie D, Susen S, Klein B, Parini A, Lamirault G, Croisille P, Rouard H, Bourin P, Nguyen JM, Delasalle B, Vanzetto G, Van Belle E, Lemarchand P.** Intracoronary autologous mononucleated bone marrow cell infusion for acute myocardial infarction: results of the randomized multicenter BONAMI trial. *Eur Heart J* 32: 1748–1757, 2011. doi:10.1093/eurheartj/ehq455.
54. **Roth GA, Johnson C, Abajobir A, Abd-Allah F, Abera SF, Abyu G, Ahmed M, Aksut B, Alam T, Alam K, Alla F, Alvis-Guzman N, Amrock S, Ansari H, Ärnlöv J, Asayesh H, Atey TM, Avila-Burgos L, Awasthi A, Banerjee A, Barac A, Bärnighausen T, Barregard L, Bedi N, Belay Ketema E, Bennett D, Berhe G, Bhutta Z, Bitew S, Carapetis J, Carrero JJ, Malta DC, Castañeda-Orjuela CA, Castillo-Rivas J, Catalá-López F, Choi JY, Christensen H, Cirillo M, Cooper L Jr, Criqui M, Cundiff D, Damasceno A, Dandona L, Dandona R, Davletov K, Dharmaratne S, Dorairaj P, Dubey M, Ehrenkranz R, El Sayed Zaki M, Faraon EJA, Esteghamati A, Farid T, Farvid M, Feigin V, Ding EL, Fowkes G, Gebrehiwot T, Gillum R, Gold A, Gona P, Gupta R, Habtewold TD, Hafezi-Nejad N, Hailu T, Hailu GB, Hankey G, Hassen HY, Abate KH, Havmoeller R, Hay SI, Horino M, Hotez PJ, Jacobsen K, James S, Javanbakht M, Jeemon P, John D, Jonas J, Kalkonde Y, Karimkhani C, Kasaeian A, Khader Y, Khan A, Khang YH, Khera S, Khoja AT, Khubchandani J, Kim D, Kolte D, Kosen S, Krohn KJ, Kumar GA, Kwan GF, Lal DK, Larsson A, Linn S, Lopez A, Lotufo PA, El Razek HMA, Malekzadeh R, Mazidi M, Meier T, Meles KG, Mensah G, Meretoja A, Mezgebe H, Miller T, Mirrakhimov E, Mohammed S, Moran AE, Musa KI, Narula J, Neal B, Ngalesoni F, Nguyen G, Obermeyer CM, Owolabi M, Patton G, Pedro J, Qato D, Qorbani M, Rahimi K, Rai RK, Rawaf S, Ribeiro A, Safiri S, Salomon JA, Santos I, Santric Milicevic M, Sartorius B, Schutte A, Sepanlou S, Shaikh MA, Shin MJ, Shishehbor M, Shore H, Silva DAS, Sobngwi E, Stranges S, Swaminathan S, Tabarés-Seisdedos R, Tadele Atnafu N, Tesfay F, Thakur JS, Thrift A, Topor-Madry R, Truelsen**

Downloaded from journals.physiology.org/journal/ajpheart (168.096.240.002) on May 3, 2021.

T, Tyrovolas S, Ukwaja KN, Uthman O, Vasankari T, Vlassov V, Vollset SE, Wakayo T, Watkins D, Weintraub R, Werdecker A, Westerman R, Wiysonge CS, Wolfe C, Workicho A, Xu G, Yano Y, Yip P, Yonemoto N, Younis M, Yu C, Vos T, Naghavi M, Murray C. Global, regional, and national burden of cardiovascular diseases for 10 causes, 1990 to 2015. *J Am Coll Cardiol* 70: 1–25, 2017. doi:10.1016/j.jacc.2017.04.052.

55. **Ruan H, Liao Y, Ren Z, Mao L, Yao F, Yu P, Ye Y, Zhang Z, Li S, Xu H, Liu J, Diao L, Zhou B, Han L, Wang L.** Single-cell reconstruction of differentiation trajectory reveals a critical role of ETS1 in human cardiac lineage commitment. *BMC Biol* 17: 89, 2019. doi:10.1186/s12915-019-0709-6.
56. **Schafer C, Young ZT, Makarewich CA, Elnwasany A, Kinter C, Kinter M, Szweda LI.** Coenzyme A-mediated degradation of pyruvate dehydrogenase kinase 4 promotes cardiac metabolic flexibility after high-fat feeding in mice. *J Biol Chem* 293: 6915–6924, 2018. doi:10.1074/jbc.RA117.000268.
57. **Schmit F, Korenjak M, Mannefeld M, Schmitt K, Franke C, von Eyss B, Gagrica S, Hänel F, Brehm A, Gaubatz S.** LINC, a human complex that is related to pRB-containing complexes in invertebrates regulates the expression of G2/M genes. *Cell Cycle* 6: 1903–1913, 2007. doi:10.4161/cc.6.15.4512.
58. **Schmittgen TD, Livak KJ.** Analyzing real-time PCR data by the comparative C(T) method. *Nat Protoc* 3: 1101–1108, 2008. doi:10.1038/nprot.2008.73.
59. **Shapiro SD, Ranjan AK, Kawase Y, Cheng RK, Kara RJ, Bhattacharya R, Guzman-Martinez G, Sanz J, Garcia MJ, Chaudhry HW.** Cyclin A2 induces cardiac regeneration after myocardial infarction through cytokinesis of adult cardiomyocytes. *Sci Transl Med* 6: 224ra27, 2014. doi:10.1126/scitranslmed.3007668.
60. **Sharma A, Zhang Y, Wu SM.** Harnessing the induction of cardiomyocyte proliferation for cardiac regenerative medicine. *Curr Treat Options Cardiovasc Med* 17: 404, 2015. doi:10.1007/s11936-015-0404-z.
61. **Siddiqi S, Sussman MA.** The heart: mostly postmitotic or mostly premitotic? Myocyte cell cycle, senescence, and quiescence. *Can J Cardiol* 30: 1270–1278, 2014. doi:10.1016/j.cjca.2014.08.014.
62. **Sonnet W, Rezsöhazy R, Donnay I.** Characterization of TALE genes expression during the first lineage segregation in mammalian embryos. *Dev Dyn* 241: 1827–1839, 2012. doi:10.1002/dvdy.23873.
63. **Takehara N, Matsubara H.** Cardiac regeneration therapy: connections to cardiac physiology. *Am J Physiol Heart Circ Physiol* 301: H2169–H2180, 2011. doi:10.1152/ajpheart.00768.2011.
64. **Tao G, Kahr PC, Morikawa Y, Zhang M, Rahmani M, Heallen TR, Li L, Sun Z, Olson EN, Amendt BA, Martin JF.** Pitx2 promotes heart repair by activating the antioxidant response after cardiac injury. *Nature* 534: 119–123, 2016. doi:10.1038/nature17959.
65. **Thornburg K, Jonker S, O'Tierney P, Chattergoon N, Louey S, Faber J, Giraud G.** Regulation of the cardiomyocyte population in the developing heart. *Prog Biophys Mol Biol* 106: 289–299, 2011. doi:10.1016/j.pbiomolbio.2010.11.010.
66. **Torrado M, Franco D, Hernández-Torres F, Crespo-Leiro MG, Iglesias-Gil C, Castro-Beiras A, Mikhailov AT.** Pitx2c is reactivated in the failing myocardium and stimulates myf5 expression in cultured cardiomyocytes. *PLoS One* 9: e90561, 2014. doi:10.1371/journal.pone.0090561.
67. **van den Brink SC, Sage F, Vértesy Á, Spanjaard B, Peterson-Maduro J, Baron CS, Robin C, van Oudenaarden A.** Single-cell sequencing reveals dissociation-induced gene expression in tissue subpopulations. *Nat Methods* 14: 935–936, 2017. doi:10.1038/nmeth.4437.
68. **Volk M, Maver A, Hodžić A, Lovrečić L, Peterlin B.** Transcriptome profiling uncovers potential common mechanisms in fetal trisomies 18 and 21. *OMICS* 21: 565–570, 2017. doi:10.1089/omi.2017.0123.
70. **Wang Z, Gerstein M, Snyder M.** RNA-Seq: a revolutionary tool for transcriptomics. *Nat Rev Genet* 10: 57–63, 2009. doi:10.1038/nrg2484.
71. **Weeland CJ, van den Hoogenhof MM, Beqqali A, Creemers EE.** Insights into alternative splicing of sarcomeric genes in the heart. *J Mol Cell Cardiol* 81: 107–113, 2015. doi:10.1016/j.yjmcc.2015.02.008.
72. **Wei W, Lv Y, Gan Z, Zhang Y, Han X, Xu Z.** Identification of key genes involved in the metastasis of clear cell renal cell carcinoma. *Oncol Lett* 17: 4321–4328, 2019. doi:10.3892/ol.2019.10130.
73. **Welch JD, Kozareva V, Ferreira A, Vanderburg C, Martin C, Macosko EZ.** Single-cell multi-omic integration compares and contrasts features of brain cell identity. *Cell* 177: P1873–P1887.E17, 2019. doi:10.1016/j.cell.2019.05.006.
74. **Wu YH, Zhao H, Zhou LP, Zhao CX, Wu YF, Zhen LX, Li J, Ge DX, Xu L, Lin L, Liu Y, Liang DD, Chen YH.** miR-134 modulates the proliferation of human cardiomyocyte progenitor cells by targeting Meis2. *Int J Mol Sci* 16: 25199–25213, 2015. doi:10.3390/ijms161025199.
75. **Xie M, Cao N, Ding S.** Small molecules for cell reprogramming and heart repair: progress and perspective. *ACS Chem Biol* 9: 34–44, 2014. doi:10.1021/cb400865w.
76. **Xie YP, Lai S, Lin QY, Xie X, Liao JW, Wang HX, Tian C, Li HH.** CDC20 regulates cardiac hypertrophy via targeting LC3-dependent autophagy. *Theranostics* 8: 5995–6007, 2018. doi:10.7150/thno.27706.
77. **Yan X, Dong N, Hao X, Xing Y, Tian X, Feng J, Xie J, Lv Y, Wei C, Gao Y, Qiu Y, Wang T.** Comparative transcriptomics reveals the role of the Toll-Like receptor signaling pathway in fluoride-induced cardiotoxicity. *J Agric Food Chem* 67: 5033–5042, 2019. doi:10.1021/acs.jafc.9b00312.
78. **Ye L, D'Agostino G, Loo SJ, Wang CX, Su LP, Tan SH, Tee GZ, Pua CJ, Pena EM, Cheng RB, Chen WC, Abdurrachim D, Lalic J, Tan RS, Lee TH, Zhang J, Cook SA.** Early Regenerative Capacity in the Porcine Heart. *Circulation* 138: 2798–2808, 2018. doi:10.1161/CIRCULATIONAHA.117.031542.
79. **Zebrowski DC, Becker R, Engel FB.** Towards regenerating the mammalian heart: challenges in evaluating experimentally induced adult mammalian cardiomyocyte proliferation. *Am J Physiol Heart Circ Physiol* 310: H1045–H1054, 2016. doi:10.1152/ajpheart.00697.2015.
80. **Zeng R, Liang Y, Farooq MU, Zhang Y, Ei HH, Tang Z, Zheng T, Su Y, Ye X, Jia X, Zhu J.** Alterations in transcriptome and antioxidant activity of naturally aged mice exposed to selenium-rich rice. *Environ Sci Pollut Res Int* 26: 17834–17844, 2019. doi:10.1007/s11356-019-05226-7.
81. **Zhang C, Wang G, Wang J, Ji Z, Dong F, Chao T.** Analysis of differential gene expression and novel transcript units of ovine muscle transcriptomes. *PLoS One* 9: e89817, 2014. doi:10.1371/journal.pone.0089817.
82. **Zhang J, Qian L, Wu J, Lu D, Yuan H, Li W, Ying X, Hu S.** Up-regulation of FAM64A promotes epithelial-to-mesenchymal transition and enhances stemness features in breast cancer cells. *Biochem Biophys Res Commun* 513: 472–478, 2019. doi:10.1016/j.bbrc.2019.03.207.
83. **Zhang J, Xue X, Xu Y, Zhang Y, Li Z, Wang H.** The transcriptome responses of cardiomyocyte exposed to hypothermia. *Cryobiology* 72: 244–250, 2016. doi:10.1016/j.cryobiol.2016.03.011.
84. **Zhang R, Lahens NF, Ballance HI, Hughes ME, Hogenesch JB.** A circadian gene expression atlas in mammals: implications for biology and medicine. *Proc Natl Acad Sci USA* 111: 16219–16224, 2014. doi:10.1073/pnas.1408886111.
85. **Zhang X, Rui L, Lv B, Chen F, Cai L.** Adiponectin Relieves Human Adult Cardiac Myocytes Injury Induced by Intermittent Hypoxia. *Med Sci Monit* 25: 786–793, 2019. doi:10.12659/MSM.912349.

Downloaded from journals.physiology.org/journal/ajpheart (168.096.240.002) on May 3, 2021.